

To appear in ApJ 511, January 20, 1999

OH 1720 MHz Masers in Supernova Remnants — C-Shock Indicators

Phil Lockett¹, Eric Gauthier^{1,2}, and Moshe Elitzur³

ABSTRACT

Recent observations show that the OH 1720 MHz maser is a powerful probe of the shocked region where a supernova remnant strikes a molecular cloud. We perform a thorough study of the pumping of this maser and find tight constraints on the physical conditions needed for its production. The presence of the maser implies moderate temperatures (50 – 125 K) and densities ($\sim 10^5 \text{ cm}^{-3}$), and OH column densities of order 10^{16} cm^{-2} . We show that these conditions can exist only if the shocks are of C-type. J-shocks fail by such a wide margin that the presence of this maser could become the most powerful indicator of C-shocks. These conditions also mean that the 1720 MHz maser will be inherently weak compared to the other ground state OH masers. All the model predictions are in good agreement with the observations.

1. Introduction

The ground state maser lines of the OH molecule have long been important sources of information about the regions in which they are formed. The main lines at 1665 and 1667 MHz and the satellite line at 1612 MHz have been widely observed in star forming regions and the envelopes of late-type stars. The satellite line at 1720 MHz has been the least commonly observed and has received the least attention until recently. However, the 1720 MHz maser is now known to be an important indicator of interactions between supernova remnants and molecular clouds. This connection was first suggested by Goss & Robinson (1968), who noted a new class of 1720 MHz masers in the supernova remnants (SNR) W28 and W44. They detected strong 1720 MHz emission, while the other ground state lines were in absorption. Little additional study of these masers was performed until recently, when the connection between 1720 MHz maser emission and SNR's was clearly established by Frail, Goss & Slysh (1994). In a followup survey, 1720 MHz maser emission was detected in 17 out of 160 SNR's (Green et al. 1997). Another source of 1720 MHz maser emission has also been discovered near the galactic center (Yusef-Zadeh et al. 1996). All

¹Centre College, 600 West Walnut Street, Danville, KY 40422; lockett@centre.edu

²Department of Physics & Astronomy, The Johns Hopkins University, 3400 North Charles Street, Baltimore, MD 21218; gauthier@pha.jhu.edu

³Department of Physics and Astronomy, University of Kentucky, Lexington, KY 40506-0055; moshe@pa.uky.edu

these masers appear to be the result of shock waves propagating perpendicular to the line of sight, hitting adjacent molecular clouds. In their comprehensive study, Frail et al. (1996) note that the maser velocities are usually close to those of the surrounding gas. This finding is corroborated by Claussen et al. (1997), who also find in the particular case of IC443 that the masers are confined to one clump of the SNR. Earlier molecular line studies by van Dishoeck, Jansen, & Phillips (1993) showed that, in that particular clump, the shock is propagating perpendicular to the line of sight. Therefore, as could be expected, the maser emission is strongest parallel to the shock front, the direction of largest velocity coherence along the line of sight.

The molecular line studies of van Dishoeck et al. (1993) also find that in IC443 the pre-shock temperature is ~ 15 K and density $\sim 10^4$ cm $^{-3}$. The corresponding postshock values are ~ 80 K and $\sim 10^5$ cm $^{-3}$, respectively. These postshock measurements are supported by the recent H $_2$ CO and CO observations of Frail & Mitchell (1998), who determined a temperature ~ 80 K and densities of $10^4 - 10^5$ cm $^{-3}$ in their study of W28, W44 and 3C391. Estimates of the post-shock OH column density in W28 range from 10^{16} to 10^{17} cm $^{-2}$ (Frail et al. 1994). Finally, Yusef-Zadeh et al. (1996), Claussen et al. (1997) and Koralesky et al. (1998) detected strong polarization and inferred magnetic fields up to a few milligauss in these maser regions.

The basic pumping mechanism for the 1720 MHz masers was identified long ago (Elitzur 1976; E76 hereafter) as collisional excitations at moderate temperatures ($T \lesssim 200$ K), densities ($n \lesssim 10^5$ cm $^{-3}$) and OH column densities ($N_{\text{OH}} \sim 10^{16}-10^{17}$ cm $^{-2}$). Here we refine these old calculations with the latest collision rates and use the constraints imposed by the pumping requirements to construct a detailed model for the masers around SNR's. In section II we discuss the collisional pumping of the 1720 MHz maser and present the results of calculations that show the effects of gas temperature, molecular density and dust radiation on the maser intensity. In section III we analyze the constraints the pumping imposes on the type of shock and present a shock model that is in good agreement with the 1720 MHz maser observations. Section IV contains our conclusions.

2. Collisional Pumping of the 1720 MHz Maser

At the low temperatures in the 1720 maser region, most of the OH molecules populate the four hyperfine levels of the ground state $^2\Pi_{3/2}(J = 3/2)$ (see figure 1). Excitations to the higher rotational levels followed by radiative cascades back to the ground reshuffle the molecules among the ground-state hyperfine levels, leading to inversion of one of the satellite lines when the final cascade is optically thick. When that final decay is from the first excited state, $^2\Pi_{3/2}(J = 5/2)$, the 1720 MHz transition is inverted. However, when the final decay is from the next excited state, $^2\Pi_{1/2}(J = 1/2)$, the 1612 Mhz line is inverted instead. As a result, the 1720 MHz inversion occurs only if the final cascade back to the ground is dominated by optically thick decays from the first excited state. This condition is met only when excitations are by collisions at $T \lesssim 200$ K, so that $^2\Pi_{3/2}(J = 5/2)$ is preferentially populated, and $N_{\text{OH}} \lesssim 10^{17}$ cm $^{-2}$, so that decays from $^2\Pi_{1/2}(J = 1/2)$ are optically thin; when N_{OH} is increased sufficiently, the inversion switches to

the 1612 Mhz line. These basic principles have been established long ago (E76) and verified in numerous observations, most notably by van Langevelde et al. (1995).

The mechanism responsible for the 1720 MHz inversion arises from the basic energy level structure of OH. In particular, it involves simple level counting and is largely independent of the specific form of collision rates; inversion should occur as long as these rates do not exhibit peculiar selection rules. Due to the lack of calculated collision rates, the E76 study employed hard sphere rates in which all downward collisions have equal strength. The calculation of actual OH collision cross sections is difficult, and the initial attempts were plagued by serious errors. These mistakes, reviewed by Flower (1990), sometimes led to completely opposite conclusions concerning the pumping of the various OH maser lines. However, the latest collision rates calculated by Offer et al. (1994) for the 24 hyperfine levels shown in figure 1 are more accurate than earlier ones and are also in reasonable agreement with experiment.

The present work utilizes the Offer et al. (1994) collision rates to update the original E76 calculations. Similar to that study, the level populations are calculated in the escape probability formalism and here we employ the expression developed by Capriotti (1965) for a quiescent slab. We have also investigated the effect of dust continuum radiation on the maser strength. The dust intensity is computed from the approximation

$$I_\nu = [1 - e^{-\tau_{\nu,d}}]B_\nu(T_d) \quad (1)$$

where $B_\nu(T_d)$ is the Planck function of the dust temperature T_d and $\tau_{\nu,d}$ is the dust optical depth with a spectral shape following the standard ISM dust cross section (Draine & Lee 1984). The calculation of the OH level populations is complicated by the phenomenon of line overlap, which occurs when the frequencies of two or more spectral lines are sufficiently close that photons emitted by one can be absorbed by another. This affects the escape of the photons and the level populations. We have incorporated the effects of overlap due to thermal motions with the aid of the method of Lockett & Elitzur (1989).

2.1. Results

We compute the populations of the 24 levels shown in figure 1 for a variety of physical parameters, assuming thermal linewidths. From the level populations we find the maser optical depth τ_m in the direction of shock propagation. The largest maser amplification will occur in the direction of largest velocity coherence and will tend to be perpendicular to the shock motion, similar to the case of water masers in star-forming regions (Elitzur, Hollenbach & McKee 1989). Our results are presented in figures (2)–(4), which display the effects of temperature, density and external radiation field on the maser. The figures show how each property affects the variation of maser optical depth τ_m with OH column density N_{OH} . Figure (2) shows the effect of gas temperature. Strong maser emission constrains the temperature to be between about 50 and 125 K, with maximum inversion occurring for $T \sim 75$ K. It is interesting to note that the upper limit

on the temperature is affected by line overlap. Without overlap, significant inversion would persist beyond 125 K, declining only when T exceeds 150 K.

Figure (3) shows the effect of molecular density. The maser cannot operate at high densities since quenching by collisions occurs at densities above about $3 \times 10^5 \text{ cm}^{-3}$. Although the inversion persists as the density decreases, very low densities are not compatible with realistic maser gains, $\tau_m \gtrsim 2$, which require $N_{\text{OH}} \gtrsim 4 \times 10^{15} \text{ cm}^{-2}$. Since the OH abundance relative to H_2 is probably no more than $\sim 10^{-5}$, the corresponding overall column density is $\gtrsim 4 \times 10^{20} \text{ cm}^{-2}$. Both observations and model calculations discussed below limit the OH shell width to less than $\sim 2 \times 10^{16} \text{ cm}$, thus the overall density in the region must exceed $\sim 10^4 \text{ cm}^{-3}$. Our calculations therefore suggest that the range of molecular densities for observable maser emission most likely lie between 10^4 and $5 \times 10^5 \text{ cm}^{-3}$.

Figure (4) presents the effect of the dust continuum radiation on the maser strength, showing that dust at a temperature $T_d = 50 \text{ K}$ has little impact on the maser effect. However, at $T_d = 100 \text{ K}$ the dust radiation diminishes significantly the maser inversion even with a minimal amount of dust. SNR's often show strong IR continuum emission which would tend to reduce the 1720 MHz maser inversion. However, observations indicate relatively low dust emission and temperatures in the maser sources IC443 and 3C391. Burton et al. (1990) find that the IR emission from IC443 is dominated by line emission rather than by dust continuum radiation. When line emission is taken into account, a dust temperature of $\sim 45 \text{ K}$ is found (van Dishoeck et al. 1993). Reach & Rho (1996) have recently measured the IR continuum emission from 3C391 using ISO and find a dust temperature of 50 K. Figure 4 shows that in these sources the dust radiation will not seriously reduce the maser inversion. Furthermore, the galactic center masers observed by Yusef-Zadeh et al. (1996) are located outside the region of intense IR emission (Mezger, Duschl, & Zylka 1996).

The results presented here are similar to those derived in E76 with hard sphere collisions, corroborating the conclusion of that study that the 1720 MHz inversion reflects the basic OH energy level structure and is largely independent of the exact form of collision rates. Because of the severe limitation on OH column density, the maser optical depth is never large. Indeed, even under optimal pumping conditions the 1720 MHz maser barely reaches saturation for radiation propagating along the shock direction; when τ_m is increased to the point that amplified maser intensity is at saturation level, N_{OH} is already so large that the inversion switches to the 1612 MHz maser. However, significant brightness temperatures can be produced for radiation propagating parallel to the shock front with amplification optical depth $a\tau_m$, where a is an aspect ratio. For $N_{\text{OH}} \sim 10^{16} \text{ cm}^{-2}$, modest aspect ratios of only 3–4 suffice to produce brightness temperatures in the range 10^8 – 10^{10} K .

Detailed OH pumping calculations based on the Offer et al. (1994) rates were also performed by Pavlakis & Kylafis (1996; PK96 hereafter), and our results are in general agreement with theirs. The Offer et al. calculations were the first to include collisions with both ortho- and para- H_2 , and PK96 found that collisions with para- H_2 can eliminate the 1720 MHz inversion. They suggested,

therefore, that the 1720 MHz maser might be used as a tool to determine the ortho-to-para ratio of molecular hydrogen. Our calculations support the PK96 finding that para-H₂ collisions do not lead to 1720 MHz inversion. However, we conclude that this inversion may not provide a useful indicator of the H₂ ortho-to-para ratio. First, an examination of the cross sections shows that the dramatic difference in maser efficiency between the ortho- and para-H₂ collisions reflects a minor peculiarity of the cross sections. Para collisions deplete the maser upper level more than the lower level while ortho collisions deplete both at roughly the same rate. This disparity arises mostly because of a single collision rate: the rate from $^2\Pi_{3/2}(J = 5/2, F = 3^+)$ to the maser’s lower level is more than 100 times smaller than that to the upper level for the para collisions. Merely setting these two rates equal to each other, as they are for the ortho collisions, produces a 1720 MHz inversion also for para-H₂. Thus the lack of a 1720 MHz maser depends sensitively on just a couple of cross sections. Although the latest rates are the most exact and complete that have yet been calculated, the history of OH collision rate calculations suggests that caution should be exercised in reaching conclusions based on selective collision rates.

A second deficiency of the 1720 MHz maser as a diagnostic of the ortho to para ratio is that it takes just a small amount of ortho to produce the maser since the relevant ortho collision rates are much larger than the para rates. The equilibrium ratio of ground state ortho to para H₂ is $9 \exp(-170/T)$. However, the ratio is predicted to be higher than the equilibrium value at low temperatures (Le Boulton 1991), indeed, observations of protostellar outflows yield a ratio of 3 ± 0.4 (Smith, Davis & Liou 1997). It is believed that H₂ forms on grains at an ortho to para ratio of 3:1, and that radiative decays preserve this ratio as the gas cools down. The results presented in figures (2)–(4) used an ortho to para ratio of 3:1. Strong 1720 MHz maser emission would persist as long as this ratio is larger than one. Although this ratio will probably influence the strength of the 1720 MHz maser, it would be difficult to estimate its value from the maser intensity alone.

3. The Maser Region — C-Shock Diagnostic

Our pumping calculations predict that the 1720 MHz maser should arise under the following conditions: $T \sim 50\text{--}125$ K, $n \sim 10^5 \text{ cm}^{-3}$, $N_{\text{OH}} \sim 10^{16}\text{--}10^{17} \text{ cm}^{-2}$. These parameters are in excellent agreement with the observations (§1), which clearly establish that the 1720 MHz masers are produced at the shock interface of a SNR with a molecular cloud. It is also significant that these conditions do not result in production of the other ground state masers. As discussed earlier (§2), the 1612 MHz maser requires a larger OH column for its creation while the main line masers require high dust temperatures (Elitzur 1992), which would destroy the 1720 MHz maser⁴. It is also important that a recent search did not detect the 22 GHz water maser in association with the

⁴This is perhaps the reason why the 1720 MHz maser is the only one of the ground state OH masers not observed in the envelopes of late-type stars.

1720 MHz maser (Claussen et al. 1998). This non-detection is significant, since observable 22 GHz water maser emission is not expected for the densities and temperatures present in these regions. We now model the environment that can generate these conditions, and show that it requires a C-type shock. Thus the production of the 1720 MHz maser can be used as a diagnostic of the shock structure.

Our conclusion that the shock must be C-type is based solely on the physical conditions necessary for 1720 MHz maser action. Because of the rapid cooling of the shocked material, the time spent in the necessary temperature range is so short that the accumulated column density is much too small to produce observable maser emission. We will show that ambipolar diffusion heating in C-shocks can overcome this rapid cooling, but that no equivalent heat source exists for J-shocks. Consider the material leaving a shock front, where it was heated to a high temperature. As this hot material streams away, it both cools and slows down so that its temperature T , velocity v , and density n are unique functions of distance l from the front. Assuming an elevated OH abundance of 10^{-5} gives a lower limit of $\sim 10^{21} \text{ cm}^{-2}$ for the H_2 column density of the maser, and the shock must be able to produce such a column for the shocked material as it cools down from $T_h \sim 125 \text{ K}$ to $T_l \sim 50 \text{ K}$. From mass conservation, the column contained between these two temperatures is (Elitzur 1980)

$$N_{\text{H}_2} = \int n dl = \int n v dt = n_0 v_s \int_{T_l}^{T_h} t_{\text{cool}} \frac{dT}{T} \quad (2)$$

where n_0 is the pre-shock density, v_s is the shock velocity and $t_{\text{cool}} = |d \ln T / dt|^{-1}$ is the cooling timescale ($= \frac{5}{2} kT / \Lambda$, where Λ is the net energy loss rate per particle). This relation is a direct consequence of mass conservation and applies to all shocks. Its evaluation requires an estimate of t_{cool} , i.e., Λ . Assume first that there is no heating in the shocked region, as is the case in standard J-shocks, then Λ is determined by the cooling processes only. Detailed calculations show that the dominant coolant in the relevant temperature region is OI, through its 3P fine structure transitions (e.g. Hollenbach & McKee 1989), and simple estimates show that $\Lambda \simeq 6 \times 10^{-25} T \text{ erg s}^{-1}$ per H_2 in this case. This gives a temperature-independent cooling timescale $\sim 6 \times 10^8 \text{ s}$, an upper limit on t_{cool} since other coolants may also contribute. Thus the previous equation becomes

$$N_{\text{H}_2} = n_0 v_s t_{\text{cool}} \ln \frac{T_h}{T_l} \lesssim 6 \times 10^{18} n_{0,4} v_6 \text{ cm}^{-2}, \quad (3)$$

where $n_{0,4} = n_0 / (10^4 \text{ cm}^{-3})$ and $v_6 = v_s / (10^6 \text{ cm s}^{-1})$. To support the 1720 MHz maser this column must be $\sim 10^{21} \text{ cm}^{-2}$, therefore the ambient density and shock velocity are constrained by

$$n_{0,4} v_6 \gtrsim 100. \quad (4)$$

Now, in a J-shock, to a good degree of approximation the ram pressure ($\propto n_0 v_s^2$) is equal to the thermal pressure of the shocked material (Elitzur 1980). Since the pumping requirements place upper limits on both the density ($n \lesssim 5 \times 10^5 \text{ cm}^{-3}$) and temperature ($T \lesssim 125 \text{ K}$) of the maser

region, it follows that its thermal pressure is bounded by $nkT \lesssim 6.25 \times 10^7 \text{ k erg cm}^{-3}$. Therefore, pressure balance across a J-shock yields

$$n_{0,4}v_6^2 \lesssim 0.3, \quad (5)$$

another constraint on n_0 and v_s . The last two constraints can be obeyed simultaneously only if $v_s \lesssim 3 \times 10^3 \text{ cm s}^{-1}$ and $n_0 \gtrsim 3 \times 10^8 \text{ cm}^{-3}$, and these two bounds are both unphysical. The upper bound on the shock velocity is two orders of magnitude less than the speed of sound, and the *lower* limit on the *pre-shock* density exceeds the *upper* limit on the *post-shock* maser density by more than three orders of magnitude. These difficulties persist for J-shocks even when the post-shock pressure is dominated not by the thermal motions but rather by a frozen-in magnetic field. Assuming flux freezing and an ambient field $B = 10^{-6}(n_0/1 \text{ cm}^{-3})^{1/2} \text{ G}$, pressure-balance across the shock yields $n_{0,4}v_6 = 0.1n_4$, where $n = 10^4 n_4 \text{ cm}^{-3}$ is the post-shock density (e.g. Hollenbach & McKee 1989). Together with equation (4) this implies $n \gtrsim 10^7 \text{ cm}^{-3}$, a lower limit exceeding the upper bound on maser density by more than an order of magnitude.

J-shocks cannot produce the relatively high column densities necessary for observable maser emission at the relatively low thermal pressures dictated by the pumping requirements of the 1720 MHz maser. The failure can be traced directly to the low column densities that these shocks produce in the relevant temperature region. From equation 3, typical ambient densities and shock velocities produce column densities that are more than two orders of magnitude smaller than required. The problem is that t_{cool} is so short, since the cooling is so fast, and can be circumvented only if some heating existed to counter the cooling and maintain the temperature in the 50–125 K range for a longer period, extending the column. One possible heat source in J-shocks is the heat of H_2 formation on grains, which can be tapped if the shock is sufficiently fast to first dissociate all molecules (Hollenbach, McKee, & Chernoff 1987). Indeed, this is the heating mechanism invoked to create the right conditions for water masers in dissociative J-shocks with pre-shock densities $\gtrsim 3 \times 10^6 \text{ cm}^{-3}$ (Elitzur et al. 1989). However, since this mechanism involves collisional de-excitation of H_2 vibrational states, its efficiency deteriorates so rapidly at lower densities and temperatures that it becomes inoperable at the conditions required here. Another possibility is radiative heating. One common method is to first radiatively heat the dust, transferring the heat to the gas by collisions. This mechanism is not feasible here because the radiation from the heated dust would destroy the maser inversion. Another radiative heat source could be ionization by the SNR x-rays, since a significant fraction of the ionization energy goes into heating. Maloney, Hollenbach & Tielens (1996) estimate that 30–40% of the ionization energy goes into heating the gas if it is primarily molecular. From the expressions they provide, the x-ray heating rate for the conditions considered here is only $\sim 10^{-27} \text{ erg s}^{-1}$ per H_2 , about 4 orders of magnitude less than the cooling rate and thus a negligible heating source.

Heating of the shocked material can be provided by ambipolar diffusion. This mechanism occurs when flux-freezing breaks down and the shock then switches to C-type. In the parameter regime relevant here, especially the magnetic fields inferred from the polarization measurements, this is the expected shock type. Indeed, in their analysis of line emission from IC443, Burton et al.

(1990) concluded that C-shocks are present in that source. Furthermore, Reach and Rho (1998a) have recently found that the brightness of the CO lines they observed in the 3C391 maser region is consistent with C-type molecular shocks with $10^4 < n_0 < 10^5 \text{ cm}^{-3}$ and $10 < v_s < 50 \text{ km s}^{-1}$.

Detailed C-shock calculations were performed by Draine, Roberge and Dalgarno (1983, DRD hereafter). They present results for a number of models that bracket the general requirements for 1720 MHz maser operation. In particular, their intermediate density model has $n_0 = 10^4 \text{ cm}^{-3}$ and $v_s = 25 \text{ km s}^{-1}$. This shock develops a region with the appropriate temperature (50–125 K) and density ($\sim 10^5 \text{ cm}^{-3}$) that extends over a distance of $\sim 10^{16} \text{ cm}$, i.e., a column density of $\sim 10^{21} \text{ cm}^{-2}$. These are just the parameters required for the 1720 MHz maser. Unfortunately, this potential maser region has virtually no OH; as is well known, molecular shocks channel into H_2O , rather than OH, essentially all the oxygen not in CO, and this is the case also with the DRD model. However, subsequent photodissociation, which was not included in the DRD calculations, can convert the water into OH. Such dissociation could be produced by the external UV radiation field as in the case of shocks around HII/OH regions (Elitzur and de Jong 1978). The relevant photodissociation rates were listed most recently by Roberge et al. (1991)

$$R(\text{H}_2\text{O}) = 3.2 \times 10^{-10} \chi \exp(-2.5\tau_V) \text{ sec}^{-1}, \quad R(\text{OH}) = 1.9 \times 10^{-10} \chi \exp(-2.5\tau_V) \text{ sec}^{-1}. \quad (6)$$

Here χ is the local enhancement of the standard interstellar UV field (Draine 1978) and τ_V is the source's optical depth at visual wavelengths. With these rates we can solve analytically for the time dependent OH and H_2O abundances of any parcel of gas after its exposure to UV radiation. Note that time t enters into the equations only in the combination $t\chi \exp(-2.5\tau_V)$. The solution for a mixture that is initially purely H_2O is displayed in figure (5), which shows the OH abundance as a fraction of the gaseous oxygen not in CO.

Another dissociation mechanism, recently advocated by Wardle et al. (1998), involves the secondary UV photons produced after X-ray absorption. With expressions from Maloney et al. (1996), this water dissociation rate is

$$R(\text{H}_2\text{O}) \simeq 5 \times 10^{-12} \frac{L_{36}}{R_{pc}^2 N_{22}} \text{ sec}^{-1} \quad (7)$$

where $10^{36} L_{36} \text{ erg s}^{-1}$ is the SNR X-ray luminosity, $R_{pc} \text{ pc}$ is the SNR radius and $10^{22} N_{22} \text{ cm}^{-2}$ is the hydrogen column attenuating the X-ray flux. The three SNRs IC443, W44 and 3C391 have $L_{36} \sim .1\text{--}2$, $R_{pc} \sim 10$ and $N_{22} \sim 0.1\text{--}1$ (Charles & Seward 1995; Rho et al. 1994; Rho & Petre 1996). These parameters yield a water dissociation rate of $\sim 10^{-13} \text{ sec}^{-1}$, about 1000 times smaller than that due to the standard ISM field. Therefore this mechanism can be neglected, unless the x-ray flux has been underestimated by more than a factor of 50.

The width of the maser region in the DRD model is $\sim 10^{16} \text{ cm}$. With a shock speed of 25 km s^{-1} , the corresponding crossing time is ~ 125 years, same as the time of the peak evident in figure 5. Thus this figure suggests that maximum OH abundance would occur for $\chi \exp(-2.5\tau_V) \sim 1$, the strength of the unattenuated standard interstellar field. However, radiation

this intense would significantly increase the electron abundance and could drastically affect the shock structure to the point that it is no longer a C-shock. DRD note that a modest change in the pre-shock electron density will not significantly affect the structure of their 10^4 cm^{-3} C-shock because most of the momentum transfer is via charged dust grains. However, the standard, unshielded interstellar field would result in an increase of the electron abundance from 10^{-7} to about 10^{-5} , and such a large increase would have a significant effect on the shock structure. Thus there are two competing constraints on the strength of the UV field: it must be strong enough to create sufficient OH, yet not so strong as to increase the electron abundance too much. A field 100 times weaker than the standard interstellar field appears to be a reasonable choice. It will increase the electron abundance by no more than an order of magnitude while producing the required amount of OH. With $\chi \exp(-2.5\tau_V) \sim 10^{-2}$, the time axis in figure 5 is stretched so that roughly 10% of the water is converted to OH in the maser region and the OH abundance is about 2×10^{-5} . These results are in good agreement with the recent observations of Reach and Rho (1998b) who detected both OH and H_2O at an abundance ratio of $\sim 1:15$ in a shocked region in 3C391. Although more accurate estimates of the OH abundance will require shock calculations that directly include photodissociation effects, this analysis shows that water photodissociation can lead to the necessary OH column density without serious effects on the shock structure.

Finally, the ambipolar diffusion process is driven by magnetic field gradients. In a C-shock these gradients are generated by the shock compression. Additionally, gradients can be produced by field curvature, an attractive possibility given the apparent maser location at the edge of an expanding SNR. A gradient characterized by length scale $\sim 10^{17} \text{ cm}$ would produce ambipolar diffusion whose heating rate is similar to that of the DRD C-shock model. Such a gradient, which could be reasonably expected at the interface of clumps overtaken by the SNR shell, would augment the C-shock heating effect even if the ionization were higher than what DRD assumed in their calculation.

4. Discussion

For many years the 1720 MHz transition was the least observed of the OH ground state maser lines. Our work shows that the inherent weakness and rarity of this maser reflect a combination of independent factors. First, because of the severe limitation on OH column density, the 1720 MMz maser optical depth is never large. Even when produced under optimal conditions, appreciable maser amplification would require radiation propagation parallel to the shock front and sizeable aspect ratios. Second, the production of this maser places tight constraints on the physical environment. Furthermore, the particular combination of physical parameters necessary for this maser is quite uncommon and only C-shocks seem capable of producing it. Third, even C-shocks are incapable of generating the optimal conditions for this maser. The OH columns produced by these shocks correspond to τ_m smaller than its potential peak value by more than a factor of 2, a significant factor in light of the steep dependence of maser emission on optical depth. Thus our

work provides a natural explanation for the low detection rate of $\sim 10\%$ found by Green et al. (1997).

While the tight constraints on the physical conditions needed for its production make for a weak 1720 MHz maser, they also make it a powerful probe of the region where it is formed. Our most significant result is that the detection of the 1720 MHz maser rules out the possibility of a J-shock; only C-shocks can produce the conditions required for this maser. This conclusion, too, is supported by the detection of high maser polarization and the magnetic fields it implies. Because of the wide margin by which J-shocks fail to produce it, the 1720 MHz maser could be one of the best discriminators of the shock type, a reliable indicator of the presence of a C-shock.

We thank E. van Dishoeck for sending us the tabulations of the Offer et al. collision rates, and D. Frail, D. Hollenbach and W. Reach for most useful comments on the original manuscript. The partial support of NASA grant NAG5-7031 is gratefully acknowledged. After completion of this work we have learned of a study by Wardle, Yusef-Zadeh & Geballe (1998) that reached similar conclusions regarding the role of C-shocks for these masers.

Appendix: Scaling

In the absence of external radiation, the level populations are determined by the following parameters: overall density n , $N_{\text{OH}}/\Delta v$ and the temperature. When the pumping is collisional and all the relevant lines are optically thick, the first two parameters enter only in the combination

$$\xi = \frac{nN_{\text{OH}}}{\Delta v}, \quad (1)$$

a scaling parameter that proved useful in the analysis of water maser pumping (Elitzur et al. 1989). Since the 1720 MHz maser, too, is collisionally pumped, we investigated the scaling properties of its inversion efficiency $\eta = (n_u - n_l)/(n_u + n_l)$. We find that to a good degree of approximation, η is indeed a function only of T and ξ , i.e., n -independent, when $\xi \gtrsim 10^{21} \text{ cm}^{-5}/\text{km s}^{-1}$ and $n \leq 3 \times 10^5 \text{ cm}^{-3}$. At smaller values of ξ we find that η remains independent of n but ξ is replaced by $N_{\text{OH}}/\Delta v$ as the relevant scaling variable. Both scaling properties can be verified analytically with the aid of a simple 8-level model of the first two rotation states, employing hard-sphere collision rates. In this model the inversion efficiency obeys

$$\eta \propto \frac{7R_{8,4}}{R_{8,4} + 4C} + \frac{5R_{7,4}}{R_{7,3} + R_{7,4} + 4C} - \frac{5R_{5,1}}{R_{5,1} + R_{5,2} + 4C} \quad (2)$$

where level numbering is in order of increasing energy (see figure 1), $R_{ij} = A_{ij}\beta_{ij}$ is the radiative decay rate and C is the (uniform) downward collision rate. Note that C depends only on T and n while R_{ij} depends only on $N_{\text{OH}}/\Delta v$. At low densities and column densities $C < R_{ij}$, therefore η depends only on R_{ij} , i.e., $N_{\text{OH}}/\Delta v$. The dependence on $N_{\text{OH}}/\Delta v$ persists as long as some of

the radiative transitions remain optically thin. As the column density increases, the radiative decay rates become smaller, due to photon trapping, and downward collisions begin to dominate. Eventually all the relevant optical depths become large and the maser efficiency becomes a function of R_{ij}/C , i.e., it scales with ξ .

Thanks to scaling, the numerical results presented here can be extended to other densities. However, because of its small phase space, the usefulness of scaling for the 1720 MHz maser is more limited than for water masers.

REFERENCES

- Burton, M.G., Hollenbach, D.J., Haas, M.R. and Erickson, E.F. 1990, ApJ, 355, 197
- Capriotti, E.R. 1965, ApJ, 142, 1101
- Charles, P.A. & Seward, F.D. 1995, Exploring the X-ray Universe (Cambridge: Cambridge)
- Claussen, M.J., Frail, D.L., Goss, W.M. & Gaume, R.A. 1997, ApJ, 489, 143
- Claussen, M. J, Goss, W. M., Frail, D. A., & Seta, M. 1998, in preparation.
- Draine, B.T. 1978, ApJS, 36, 595
- Draine, B.T. & Lee, H.M. 1984, ApJ, 285, 89
- Draine, B.T., Roberge, W.G., Dalgarno, A. 1983, ApJ, 264, 485 (DRD)
- Elitzur, M. 1976, ApJ, 203, 124 (E76)
- Elitzur, M. 1980, A&A, 81, 351
- Elitzur, M. 1992, Astronomical Masers (Dordrecht: Kluwer)
- Elitzur, M. & deJong, T. 1978, A&A, 67, 323
- Elitzur, M., Hollenbach, D.J., McKee, C.F. 1989, ApJ, 346, 983
- Flower, D. 1990, Molecular Collisions in the Interstellar Medium (Cambridge: Cambridge)
- Frail, D.L., Goss, W.M., & Slysh, V.I. 1994, ApJ, 424, L111
- Frail, D.L., Goss, W.M., Reynoso, E.M., Giacani, E.B., Green, A.J., & Otrupcek, R. 1996, AJ, 111, 1651
- Frail, D.L., & Mitchell, G.F. 1998 ApJ, submitted
- Goss, W.M., & Robinson, B.J. 1968, Astrophys. Lett., 2, 81
- Green, A.J., Frail, D.A, Goss, W.M., & Otrupcek, R. 1997, AJ, 114, 2058
- Hollenbach, D.J. & McKee, C.F. 1989, ApJ, 342, 306
- Hollenbach, D.J., McKee, C.F. & Chernoff, D. 1987, in Star Forming Regions, eds. M. Peimbert and J. Jugaku (Dordrecht: Reidel), p. 334.

- Koralesky, B., Frail, D.A., Goss, W.M., Claussen, M.J., Green, A.J. 1998, AJ, in press
- LeBourlot, J. 1991, A&A, 242, 235
- Lockett, P. & Elitzur M. 1989, ApJ, 344, 525
- Maloney, P.R., Hollenbach, D.J. & Tielens, A.G.G.M. 1996 ApJ, 466,561
- Mezger, P.G., Duschl, W.J., & Zylka, R. 1996, A&A Rev., 7, 289
- Offer, A.R., van Hemert, M.C., & van Dishoeck, E.F. 1994, J. Chem. Phys., 100, 362
- Pavlakis, K.G. & Kylafis, N.D. 1996, ApJ, 467, 300 (PK96)
- Reach, W.T & Rho, J. 1996, A&A, 315, L277
- Reach, W.T & Rho, J. 1998a, ApJ, submitted
- Reach, W.T & Rho, J. 1998b, ApJ, submitted
- Rho, J., Petre, R., Schlegel, E. M., & Hester, J. J. 1994, ApJ, 430, 757
- Rho, J. H. & Petre, R. 1996, ApJ, 467, 698
- Roberge, W.G., Jones. D., Lepp, S., Dalgarno, A. 1991, ApJS, 77, 287
- Smith M.D., Davis, C.J., Lioure, A. 1997, A&A, 327, 1206
- van Dishoeck, E.F., Jansen, D.J., Phillips, T.G. 1993, A&A, 279, 541
- van Langevelde, H.J., van Dishoeck, E.F., Sevenster, M.N., Israel, F.P. 1995, ApJ, 448, L123
- Wardle, M., Yusef-Zadeh, F. & Geballe, T.R. 1998, preprint LANL astro-ph/9804146
- Yusef-Zadeh, F., Roberts, D.A., Goss, W.M., Frail, D.A., Green, A.J. 1996, ApJ, 466, L25

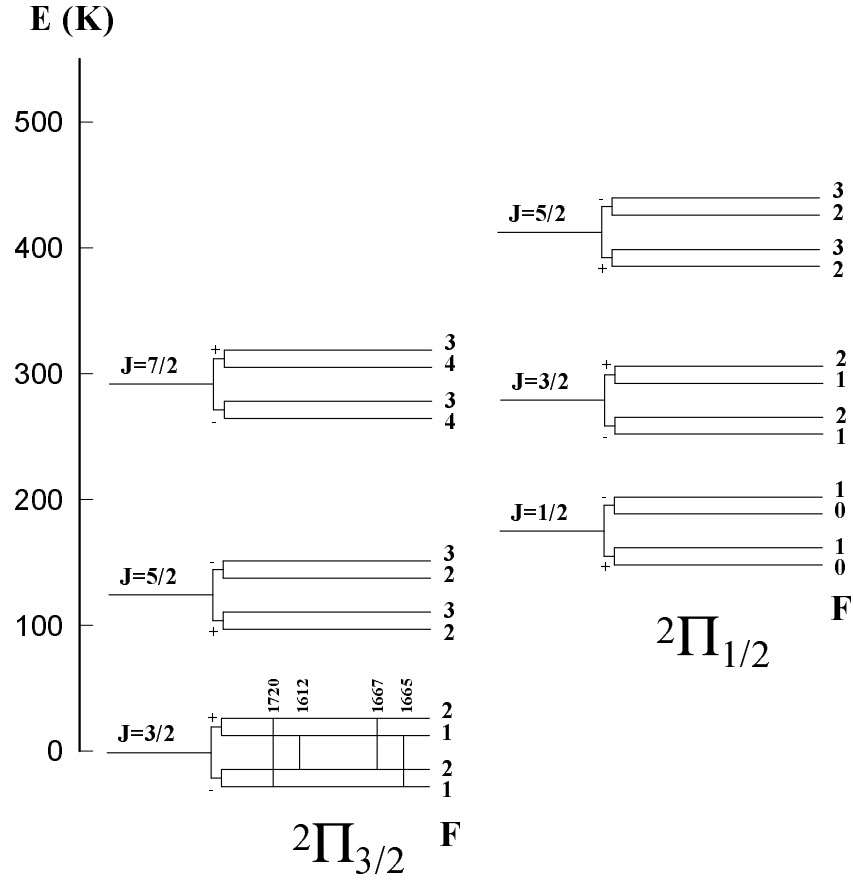


Fig. 1.— Hyperfine-rotation levels of OH used in our calculations.

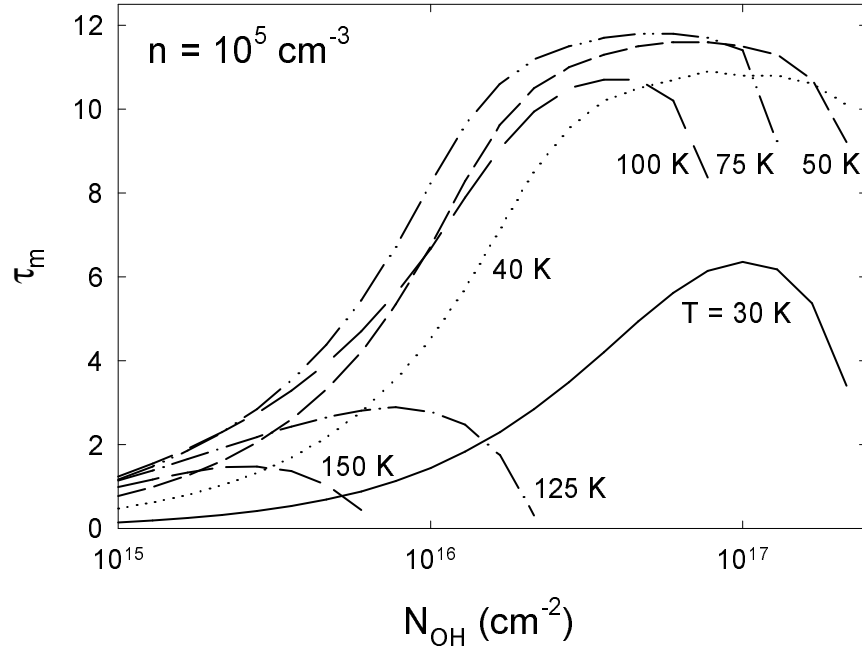


Fig. 2.— Maser optical depth as a function of OH column density for various temperatures, as marked, at density $n = 10^5 \text{ cm}^{-3}$.

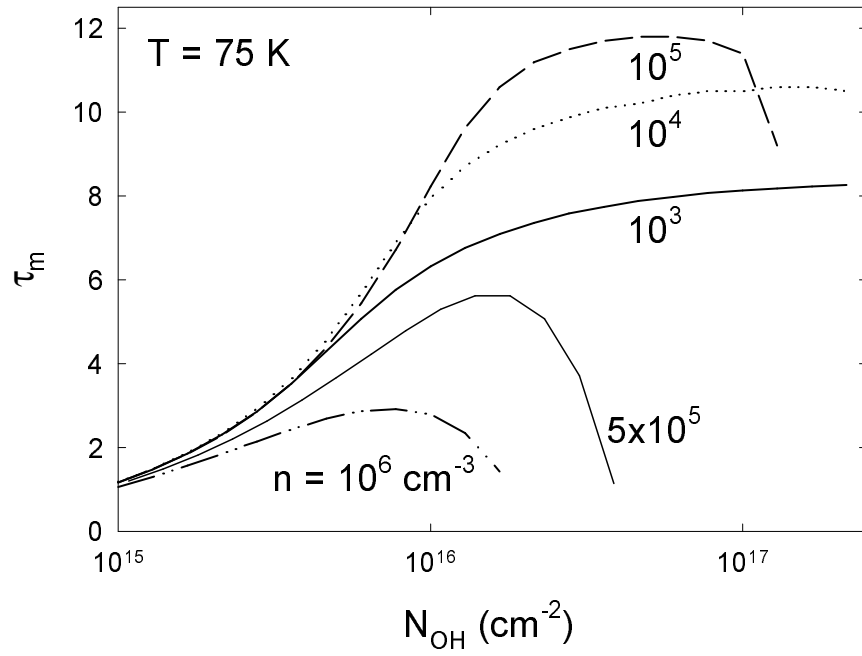


Fig. 3.— Maser optical depth as a function of OH column density for various densities, as marked, at temperature $T = 75 \text{ K}$.

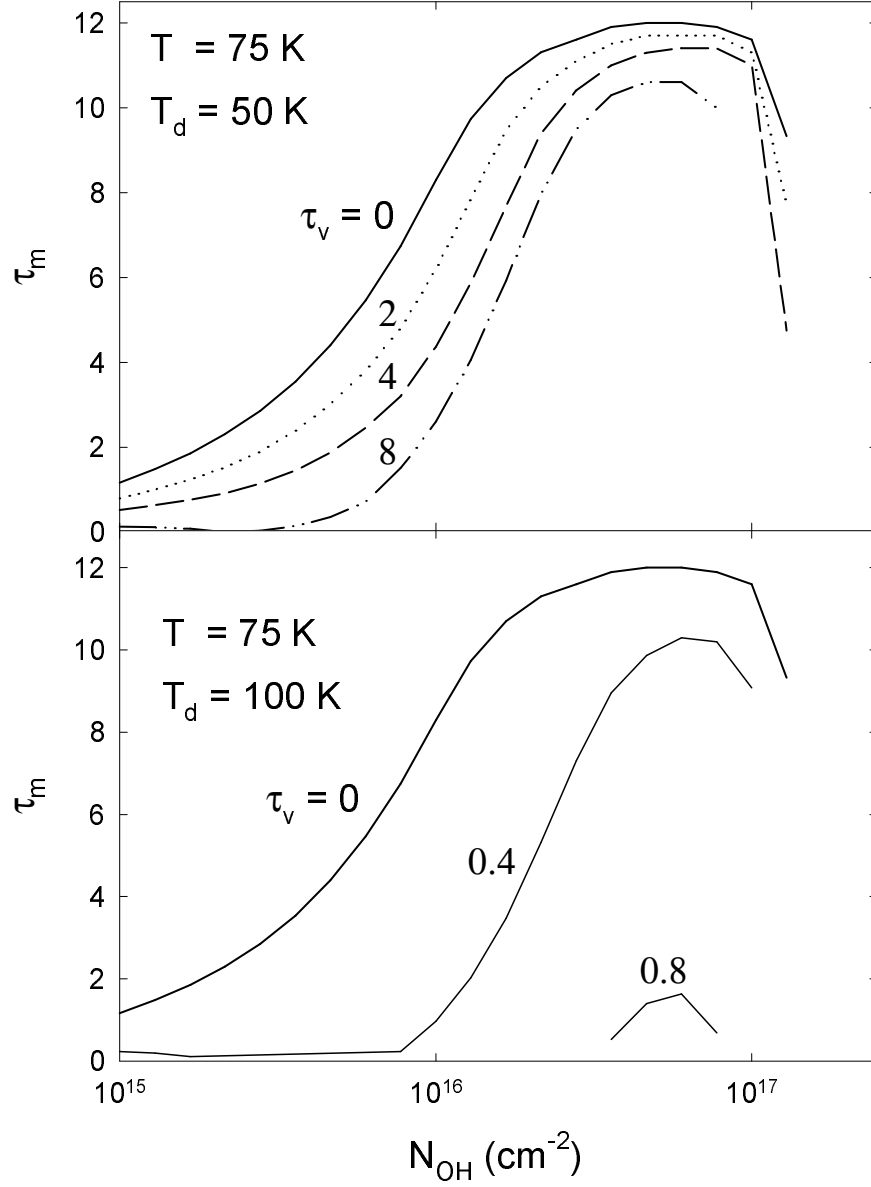


Fig. 4.— Effect of dust radiation on maser inversion: maser optical depth as a function of OH column density for various values of τ_v , the dust optical depth at visual, as marked. The dust temperature is 50 K in the top panel, 100 K in the bottom panel. In both panels, the gas has a density of 10^5 cm^{-3} and temperature 75 K. The plots for $\tau_v = 0$ are the same as the corresponding ones in figures (2) and (3) and are included for reference, to show the inversion in the absence of dust.

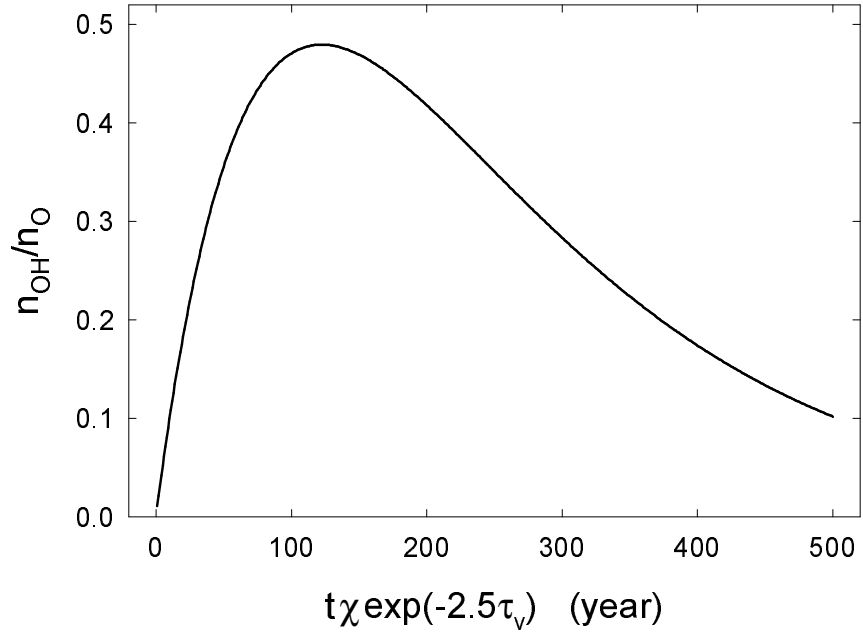


Fig. 5.— Fraction of oxygen in OH as a function of time for gas exposed to UV radiation. Initially, all oxygen is in H_2O . χ is the enhancement of the local radiation field over its standard ISM value and τ_v is the cloud’s visual extinction. The scaling properties of the time axis directly reflect the form of the photodissociation rates (eq. 6).